Journal of Controlled Release 199 (2015) 156–167

Contents lists available at ScienceDirect

Journal of Controlled Release

journal homepage: www.elsevier.com/locate/jconrel

A thermo-responsive protein treatment for dry eyes

Wan Wang [a], Aarti Jashnani [a], Suhaas R. Aluri [a], Joshua A. Gustafson [a], Pang-Yu Hsueh [a], Frances Yarber [a], Robert L. McKown [b], Gordon W. Laurie [c], Sarah F. Hamm-Alvarez [a,d], J. Andrew MacKay [a,e,*]

[a] Department of Pharmacology and Pharmaceutical Sciences, University of Southern California, Los Angeles, CA, United States
[b] Department of Integrated Science and Technology, James Madison University, Harrisonburg, VA, United States
[c] Department of Cell Biology, School of Medicine of the University of Virginia, Charlottesville, VA, United States
[d] Department of Physiology and Biophysics, Keck School of Medicine of the University of Southern California, Los Angeles, CA, United States
[e] Department of Biomedical Engineering, University of Southern California, Los Angeles, CA, United States

ARTICLE INFO

Article history:
Received 26 April 2014
Accepted 17 November 2014
Available online 3 December 2014

Keywords:
Elastin-like polypeptides (ELPs)
Lacritin
Lacrimal gland
Thermo-responsive
Prosecretory
Uptake

ABSTRACT

Millions of Americans suffer from dry eye disease, and there are few effective therapies capable of treating these patients. A decade ago, an abundant protein component of human tears was discovered and named lacritin (Lacrt). Lacrt has prosecretory activity in the lacrimal gland and mitogenic activity at the corneal epithelium. Similar to other proteins placed on the ocular surface, the durability of its effect is limited by rapid tear turnover. Motivated by the rationale that a thermo-responsive coacervate containing Lacrt would have better retention upon administration, we have constructed and tested the activity of a thermo-responsive Lacrt fused to an elastin-like polypeptide (ELP). Inspired from the human tropoelastin protein, ELP protein polymers reversibly phase separate into viscous coacervates above a tunable transition temperature. This fusion construct exhibited the prosecretory function of native Lacrt as illustrated by its ability to stimulate β-hexosaminidase secretion from primary rabbit lacrimal gland acinar cells. It also increased tear secretion from non-obese diabetic (NOD) mice, a model of autoimmune dacryoadenitis, when administered via intra-lacrimal injection. Lacrt ELP fusion proteins undergo temperature-mediated assembly to form a depot inside the lacrimal gland. We propose that these Lacrt ELP fusion proteins represent a potential therapy for dry eye disease and the strategy of ELP-mediated phase separation may have applicability to other diseases of the ocular surface.

1. Introduction

The lacrimal gland–corneal axis plays a critical role in maintaining ocular surface health. While the avascular cornea serves as both a protective barrier and the main refractive element of the visual system, the lacrimal gland (LG) is the major organ secreting key proteins and electrolytes into the tear film that bathes the cornea and, through nutrient and antimicrobial proteins, sustains its function [1,2]. Dry eye disease (DED) is a multifactorial disease of the ocular surface causing visual disturbance and tear film instability [3] and can be due to either aqueous tear insufficiency originating with defects in aqueous tear production by the LG [4] or evaporative dry eye associated with meibomian gland insufficiency [5,6]. According to reports, severe DED affects approximately 5 million Americans above age 50 and its global prevalence ranges from 5% to 35% of the population [3]. Traditional approaches to treat DED include topical administration of artificial tears or the conservation of secreted tears using tear plugs [7] and eye-shields [8]. Since many cases of DED are associated with inflammation [9,10], some treatments for DED have been proposed that inhibit inflammation of the LG [11]. None of these methods are satisfactory in replacing the lost regulatory functions provided by the many components found in normal tears. To better sustain the health and homeostasis of the ocular surface there remains a need for efficient, sustained and targeted DED therapy. In humans, the inferior palpebral lobe of the LG is accessible for injection beneath the eyelid; furthermore, if coupled with a sustained release strategy this route of administration might have clinical relevance, similar to intra-vitreal injection or subconjunctival injection.

The discovery of the glycosylated human tear protein, lacritin (Lacrt), provided critical insight into the potential use of regulatory tear proteins to treat DED [12,13]. Lacrt was found in a systematic oligonucleotide screen of a human LG cDNA library and exhibited LG specific-expression [14]. Subsequent studies have proven its efficacy in stimulating peroxidase secretion in cultured rat [14], and both lactoferrin and lipocalin secretion in cultured monkey lacrimal acinar cells [15]. Lacrt also promotes constitutive tear secretion by New Zealand white rabbits and Aire KO mice via topical treatment [16,17], proliferation of transformed human corneal epithelial cells [14,18], and restored health of

Abbreviations: DED, dry eye disease; ELP, elastin-like polypeptide; Lacrt, lacritin; T_t, transition temperature; LG, lacrimal gland; LGACs, lacrimal gland acinar cells; NOD, non-obese diabetic; CCh, carbachol.

* Corresponding author at: Department of Pharmacology and Pharmaceutical Sciences, University of Southern California, Los Angeles, CA 90033-9121, United States.
E-mail address: jamackay@usc.edu (J.A. MacKay).

http://dx.doi.org/10.1016/j.jconrel.2014.11.016
0168-3659/

transformed human corneal epithelial cells, primary human corneal epithelial cells [19] and primary monkey lacrimal acinar cells [15] that had been stressed with the inflammatory cytokines interferon-γ and tumor necrosis factor. Interestingly, Lacrt displays growth factor-like behavior; however, its specificity for target cells of the ocular surface system results from a unique 'off–on' switch controlled by heparanase deglycanation of the cell surface protein, syndecan-1 [20], which both exposes and generates a Lacrt binding site [21] as a prerequisite for mitogenic signaling. Confirmed by 2-D electrophoresis, mass spectrometry and surface-enhanced laser desorption/ionization studies, Lacrt [22] is down regulated in blepharitis (chronic inflammation of the eyelid) vs. normal tears [23], and most aqueous deficient dry eye [24]. Whether down regulation of Lacrt provokes disease is a key unresolved question, but its prosecretory and corneal mitogenic activity suggest that it might have activity as a protein therapeutic for ocular surface diseases.

Great strides have been made to improve the bioavailability and simplify the administration of existing drugs, which include depot formulations that deliver short peptides such as leuprolide and bioadhesive polymers used in buccal drug-delivery systems [25]. Recently, stimuli-responsive polypeptides have emerged as an attractive controlled release strategy. One such type of biomaterial is the elastin-like-polypeptide (ELP) [26]. Biologically inspired from human tropoelastin, ELPs are composed of a pentapeptide repeat $(VPGXG)_n$, where the 'guest residue' *X* can be any amino acid and *n* determines molecular weight. One unique property of ELPs is their inverse phase transition temperature behavior. ELPs are soluble in aqueous solutions below their transition temperature (T_t) and self-assemble into various-sized particles above T_t [27]. T_t can be precisely modulated by adjusting the number of pentapeptide repeats, *n*, and the hydrophobicity of the guest residue, *X*, which can determine whether the ELP remains a soluble macromolecular drug carrier [28], assembles a nanoparticle [29], or phase separates into micron-sized coacervates [30] at physiological temperatures. With their distinctive thermo-responsive, elastic, and biocompatible properties, ELPs have impacted fields such as protein purification [31], stimuli responsive hydrogels [32], tissue engineering [33,34], and targeted cancer treatment [35,36]. Yet, the application of ELPs in ophthalmology has just started [37,38].

To explore the concept of a thermo-responsive drug reservoir as a potential novel treatment for DED [7], we generated a novel Lacrt–ELP fusion with T_t below physiological temperature. The construct exhibits thermo-responsiveness of the parent ELPs while retaining prosecretory efficacy of native Lacrt, as demonstrated by its ability to stimulate dose-dependent β-hexosaminidase secretion from primary rabbit lacrimal gland acinar cells (LGACs). Moreover, the Lacrt–ELP fusion enhanced tear secretion from the non-obese diabetic (NOD) mouse model of autoimmune dacryoadenitis when given via intra-lacrimal injection. This treatment formed a depot that lasted over 24 h inside the LG, which was confirmed by confocal laser scanning microscopy. Finally, we captured the intracellular trafficking and transcytosis of exogenous Lacrt in LGACs using time-lapse confocal fluorescence microscopy, which was prolonged by fusion to the ELP. These findings support the potential enhancement of Lacrt therapeutics via the linkage to a thermo-responsive ELP, which may have broader implications in the treatment of DED.

2. Material and methods

2.1. Animals

In vitro studies were conducted using LG from Female New Zealand White rabbits (2.2–2.5 kg) obtained from Irish Farms (Norco, CA). *In vivo* studies were conducted using LG isolated from 12-week old male/female C57BL/6 (Jackson Labs, Bar Harbor/ME, USA) or in house bred non-obese diabetic (NOD) (Taconic Farms, Germantown/NY, USA) mice. All procedures performed were in accordance to the university approved IACUC protocol.

2.2. Instruments and reagents

Terrific broth dry powder growth medium was purchased from MO BIO Laboratories, Inc. (Carlsbad, CA). Isopropyl β-D-1-thiogalactopyranoside, OmniPur*. 99.0% min. was purchased from VWR (Visalia, CA). Amicon Ultra concentrators were purchased from Millipore (Billerica, MA). Thrombin CleanCleave™ Kit, carbachol (CCh) and insulin–transferrin–sodium selenite media supplement were purchased from Sigma-Aldrich (St. Louis, MO). 4–20% Tris-Glycine PAGEr gels were purchased from LONZA (Allendale, NJ). Cell culture reagents were from Life-Technologies (Carlsbad, CA). Peter's Complete Medium (PCM) consisted of 50% Ham's F-12 plus 50% DME (low glucose) supplemented with penicillin (100 U/ml), streptomycin (0.1 mg/ml), glutamine (4 mM), hydrocortisone (5 nM), transferrin (5 μg/ml), insulin (5 μg/ml), butyrate (2 mM), linoleic acid (0.084 mg/l), carbachol (1 μM), laminin (5 mg/l) and insulin–transferrin–sodium selenite (ITS) media supplement (5 μg/ml).

2.3. Biosynthesis of Lacrt–ELP fusions

A sequence encoding human Lacrt without a secretion signal peptide was designed using the best *Escherichia coli* codons in EditSeq (DNAStar Lasergene, WI) [39]. A thrombin cleavage site was encoded between the Lacrt sequence and ELP tag via insertion at the *BseRI* site. A custom gene flanked by *NdeI* and *BamHI* restriction digestions sites at the 5′ and 3′ ends was purchased in the pIDTSmart-KAN vector from Integrated DNA Technologies (IDT) as follows:

5′-**CATATG**GAAGACGCTTCTTCTGACTCTACCGGTGCTGACCCGGCTC
AGGAAGCTGGTACCTCTAAACCGAACGAAGAAATCTCTGGTCCGGCTG
AACCGGCTTCTCCGCCGGAAACCACCACCACCGCTCAGGAAACCTCTG
CTGCTGCTGTTCAGGGTACCGCTAAAGTTACCTCTTCTCGTCAGGAAC
TGAACCCGCTGAAATCTATCGTTGAAAAATCTATCCTGCTGACCGAAC
AGGCTCTGGCTAAAGCTGGTAAAGGTATGCACGGTGGTGTTCCGGGTG
GTAAACAGTTCATCGAAAACGGTTCTGAATTCGCTCAGAAACTGCTGA
AAAAATTCTCTCTGCTGAAACCGTGGGCTGGTCTGGTTCCGCGTGGTT
CTGGTTACTGATCTCCTC**GGATCC**-3′.

The gene encoding for V96 was synthesized by recursive directional ligation in a modified pET25b(+) vector as previously reported [40,41]. The Lacrt-thrombin gene was subcloned into the pET25b(+) vector between the *NdeI* and *BamHI* sites. LV96 gene fusions were synthesized by ligation of a gene encoding for the ELP V96 via the *BseRI* restriction site, resulting in placement of the thrombin cleavage site between Lacrt and ELP. Correct cloning of the fusion protein gene was confirmed by DNA sequencing. The amino acid sequences of ELPs used in this study are described in Table 1.

2.4. Expression and purification of Lacrt ELP fusion protein

Plain ELP V96 and the Lacrt fusion LV96 were expressed in BLR (DE3) *E. coli* (Novagen Inc., Milwaukee, WI). Briefly, V96 was expressed for 24 h in an orbital shaker at 37 °C at 250 rpm. For LV96, 500 μM Isopropyl β-D-1-thiogalactopyranoside (IPTG) was added to the culture when the OD 600 nm reached 0.5, at which point the temperature was decreased to 25 °C for protein expression for 3 h. Cell cultures were harvested and re-suspended in phosphate buffer saline (PBS). Proteins were purified from the clarified cell supernatant by inverse transition cycling [39] until ELP purity was determined to be approximately 99% by SDS-PAGE stained with $CuCl_2$. Due to partial proteolysis of LV96 during biosynthesis, fusion proteins were further purified to homogeneity using a Superose 6 (GE Healthcare Bio-Sciences, Piscataway, NJ) size exclusion column at 4 °C. After equilibration with PBS (pH 7.4), 10 mg LV96 was loaded onto the column and washed out by isocratic flow of PBS at 0.5 ml/min. P1, representing LV96 (Supplementary Fig. S1), was collected and concentrated using an Amicon Ultra

Table 1
Nomenclature, amino acid sequence, and phase behavior of expressed proteins.

Protein label	Amino acid sequence[a]	M.W.		Phase behavior[b]	
		Exp[c] [kDa]	Obs[d] [kDa]	Intercept, b [°C]	Slope, m[°C] $[\mathrm{Log}_{10}(\mu M)]^{-1}$
V96	$G(VPGVG)_{96}Y$	39.6	39.5	36.1	3.25
LV96	GEDASSDSTGADPAQEAGTSKPNEEISGPAEPASPPETTTTAQETSAAAVQGTAKVTSSRQELNPLKSIVE KSILLTEQALAKAGKGMHGGVPGGKQFIENGSEFAQKLLKKFSLLKPWAGLVPRGSG$(VPGVG)_{96}Y$	52.5	52.3	28.6	1.19
Lacrt	GEDASSDSTGADPAQEAGTSKPNEEISGPAEPASPPETTTTAQETSAAAVQGTAKVTSSRQELNPLKSIVE KSILLTEQALAKAGKGMHGGVPGGKQFIENGSEFAQKLLKKFSLLKPWAGLVPR	12.8	12.7	NA	NA

Not applicable (NA).
[a] After the start codon, a glycine spacer was added during cloning, which is not present on human Lacrt.
[b] ELPs in PBS phase separate above a line with slope m and intercept b as defined by Eq. (1).
[c] Expected M.W. was estimated for each sequence, which excludes the methionine start codon.
[d] Observed M.W. was measured by MALDI-TOF.

concentrator (10 kD). When desired, free Lacrt was released by thrombin cleavage of LV96 fusion protein. Briefly, 300 μl of thrombin bead slurry (Sigma-Aldrich) was added to 200 mg of purified LV96 and incubated at room temperature for 3 h. After pelleting the thrombin beads at 250 rpm, the solution was warmed up to 37 °C and centrifuged at 4000 rpm for 10 min to remove ELP coacervates. The supernatant was then concentrated using an Amicon Ultra concentrator with a 3 kD M.W. cut-off (MWCO). Protein concentrations were determined by UV–VIS spectroscopy at 280 nm ($\varepsilon_{ELP} = 1285\ M^{-1}\ cm^{-1}$, $\varepsilon_{LV96} = 6990\ M^{-1}\ cm^{-1}$, $\varepsilon_{Lacrt} = 5500\ M^{-1}\ cm^{-1}$). Protein molecular weight was further confirmed by MALDI-TOF mass spectrometry (AXIMA Assurance, Shimadzu).

2.5. Thermal characterization of Lacrt ELP fusion proteins

Self-assembly of purified V96 and LV96 fusion proteins was characterized by optical density using a DU800 UV–VIS spectrophotometer outfitted with the High Performance Transport and Peltier Temperature-Controlled Cell Holder (Beckman Coulter, Brea, CA). Consistent with previous reports [27,28,36], optical density was measured at 350 nm as a function of temperature, a wavelength at which LV96 and V96 contribute little absorption. ELPs (5 to 100 μM) were observed in PBS under a temperature gradient of 1 °C/min (10 to 45 °C). The cuvette provides minimal insulation between the sample and the cell holder. At this slow temperature gradient, the sample and cell holder are engineered to remain in close agreement to avoid over or under heating. The inverse transition temperature (T_t) of each solution was defined as the temperature at which the first derivative of the optical density with respect to the temperature reached a maximum. The ELP transition temperature has been observed as a function of concentration as follows:

$$T_t = b - m\mathrm{Log}_{10}[C_{ELP}] \quad (1)$$

where b is the intercept at a concentration of 1 μM ELP, m is the slope, and C_{ELP} is the ELP concentration. Eq. (1) was fit to data obtained for V96 and LV96 (Table 1).

2.6. Dynamic light scattering

To characterize the assembly process of LV96 coacervates, the hydrodynamic radius (R_h) was monitored as a function of temperature. Samples were suspended (25 μM) in PBS and were filtered through Whatman Anotop 10 syringe filters with a pore size of 0.02 μm (GE Healthcare Bio-Sciences, Piscataway, NJ) at 4 °C. Light scattering data were collected at regular temperature intervals (1 °C) as solutions were heated from 5 to 60 °C using a DynaPro-LSR Plate Reader (Wyatt Technology, Santa Barbara, CA). The results were then analyzed using a Rayleigh sphere model.

2.7. Stability of Lacrt

To determine the cleavage half-life of Lacrt, the purified proteins (20 μg) were incubated in PBS at 37 °C for 72 h followed by SDS-PAGE analysis. Peptide sequence analysis was performed using MALDI-TOF (AXIMA Assurance, Shimadzu). Cleavage products were assigned by MALDI-TOF mass by comparison of measured with predicted mass to charge ratios (m/z) with +1 charge ionization ($[M + H]^+$). For Western blotting of purified Lacrt, 50 μg purified protein was loaded onto 4–20% Tris–HCl polyacrylamide gels; with blocking buffer at room temperature for 1 h and blotted with rabbit anti-N-terminal or anti-C-terminal (1:200) Lacrt antibody [42] overnight at 4 °C followed by blotting with IRDye800 Donkey anti-rabbit IgG (H + L) (Rockland) (1:3000) at room temperature for 1 h. Images were taken using the Odyssey infrared imaging system (Li-Cor, Lincoln, NE).

2.8. Cell isolation, culture and treatments

Isolation of primary cultured LGAC from female New Zealand white rabbits was performed in accordance with the Guiding Principles for Use of Animals in Research. Specifically, LGACs were isolated from rabbit LGAC and cultured by the method of da Costa [43] in Peter's Complete Medium (PCM) medium for 2–3 days.

2.9. Secretion of β-hexosaminidase

Fresh PCM medium was added to wells containing LGAC and incubations were continued for an additional 2 h. Baseline samples were then taken from each well, and the cells were stimulated with 100 μM carbachol (CCh), Lacrt, V96, or LV96 at various concentrations as indicated for 1 h. After stimulation, the cell supernatant was collected and β-hexosaminidase activity in each aliquot was measured against a model substrate, methylumbelliferyl-N-acetyl-β-D-glucosaminide. Assays of catalytic activity were performed in 96-well plates, and reaction product absorbance was determined with a plate reader at 460 nm (Tecan Genios Plus; Phenix Research Products, Candler, NC); signals were analyzed with the manufacturer's software package (Magellan v6.6; Phenix Research Products). Medium was then aspirated from all wells and 500 μl 0.5 M NaOH was added into each well and incubated at 4 °C for overnight to lyse the acini and solubilize all protein. Total protein in each well was measured by the bicinchoninic acid assay (BCA) assay using a bovine serum albumin standard curve. Secreted β-hexosaminidase level was expressed as ΔOD465 nm (post–pre)/μg total protein. Each treatment was performed in triplicate and these assays were repeated 3 times. The secretion was normalized to the secretion induced by CCh as follows:

$$\beta\mathrm{hex}_{Secretion} = \frac{\beta\mathrm{hex}_{Treatment} - \beta\mathrm{hex}_{CCh-}}{\beta\mathrm{hex}_{CCh+} - \beta\mathrm{hex}_{CCh-}} 100\% \quad (2)$$

where $\beta hex_{Treatment}$ is the sample activity, βhex_{CCh-} is the activity released in the absence of stimulation, and βhex_{CCh+} is the activity released upon stimulation with CCh.

2.10. Live cell imaging of actin remodeling

LifeAct-RFP adenovirus was generated as described previously [44]. For amplification, QB1 cells, a derivative of HEK293 cells, were infected with the virus and grown at 37 °C and 5% CO_2 in Dulbecco's Modified Eagle's Medium (DMEM, high glucose) containing 10% fetal bovine serum for 66 h until completely detached from the flask surface. The Adeno-X™ virus purification kit (Clontech, CA) was used for virus purification and the Adeno-X™ rapid titer kit for viral titration. LGACs were transduced at a multiplicity of infection of 8–10 for 2 h at 37 °C and then rinsed and cultured in fresh medium overnight to allow for protein expression. Live cell images upon Lacrt/LV96 stimulation were captured using a Zeiss LSM 510 Meta confocal fluorescence microscopy system.

2.11. Cellular uptake of Lacrt and Lacrt ELP fusion proteins

Lacrt, V96 and LV96 were conjugated with NHS-rhodamine (Thermo Fisher Scientific Inc, Rockford, IL) via covalent modification of the amino terminus. Conjugation was performed in 100 mM borate buffer (pH 8.0) for 2 h (LV96 and Lacrt) or overnight (V96) at 4 °C followed by desalting on a PD10 column (GE Healthcare Bio-Sciences, Piscataway, NJ) to remove free dye. Degree of labeling was estimated following the manufacturer's instructions as follows:

$$C_{rhodamine} = \frac{A_{555}}{\varepsilon_{rhodamine}} \quad (3)$$

$$C_{protein} = \frac{A_{280} - (A_{555} CF_{rhodamine})}{\varepsilon_{protein}} \quad (4)$$

where $\varepsilon_{rhodamine} = 80{,}000\ M^{-1}\ cm^{-1}$; $CF_{rhodamine} = 0.34$. Cellular uptake was studied on 35 mm glass coverslip-bottomed dishes. Briefly, after washing with warm fresh medium, LGACs were cultured in medium containing 10 μM of proteins conjugated with rhodamine. After incubation at 37 °C for different time points, the cells were rinsed three times with room temperature medium and images were acquired using confocal fluorescence microscopy. The washing step does not conserve coacervate particles, which are disrupted below 27 °C, but does enable the observation of their intracellular uptake and trafficking.

2.12. Intra-lacrimal administration, retention, and tear secretion in mice

For intra-lacrimal injection, mice were anesthetized with an i.p. injection of xylazine/ketamine (60–70 mg + 5 mg/kg), administered a subcutaneous injection of buprenorphine (0.02 mg/kg), and placed on a heating pad. After removing fur from the cheek and cleansing the area with alcohol, a small incision (5 mm) was made to visualize the LG. 5 μl of 50 μM carbachol (CCh), 100 μM LV96, 100 μM V96 or 100 μM Lacrt was injected into the LG using a 33 gauge blunt needle. The mice were monitored on the heating pad until fully recovered from anesthesia. For quantification of tear secretion, a glass capillary (Microcaps Drummond disposable micropipettes 2 μl) was placed on the lower eyelid of the mice to collect tears (2 LG/each mouse, 30 min/each gland). To evaluate protein retention in the LG after intra-lacrimal injection, the incision was closed with a 6.0 synthetic suture (MERSILENE® Polyester Fiber Suture, ETHICON). Mice were euthanized after different time points, and LG were processed in one of two ways: i) fixed in 4% paraformaldehyde and 4% sucrose in PBS for 2–3 h at room temperature followed by cryoprotection in 30% sucrose at 4 °C overnight before freezing the sample in O.C.T. for immunohistochemistry analysis; ii) fixed overnight in 10% neutral buffered formalin and transferred to 70% ethanol for paraffin-embedded histology and staining by hematoxylin and eosin.

2.13. Statistical analysis

All experiments were replicated at least three times. Values are expressed as the mean ± SD. For β-hexosaminidase secretion, data were analyzed using two-way ANOVA followed by the Bonferroni post-hoc analysis (GraphPad Prism). Within each experiment, each treatment was performed in triplicate and three independent experiments have been performed ($n = 9$). For LGAC uptake studies, treatments were performed in triplicate and three representative acini in each plate were evaluated ($n = 9$). Data were then analyzed using two-way ANOVA followed by Tukey's post-hoc test (GraphPad Prism). For mouse tear secretion studies, each treatment was performed on three mice and three independent experiments were performed ($n = 9$). The results were analyzed using one-way ANOVA followed by Tukey's post-hoc test (GraphPad Prism). To evaluate protein retention in the LG, each time point was repeated in three LGs and a representative image was shown. Three sections from each sample were imaged and quantified using ImageJ ($n = 9$). Data were then analyzed using two-way ANOVA followed by the Bonferroni post-hoc analysis (GraphPad Prism). A p value less than 0.05 was considered statistically significant.

3. Results

3.1. Construction and purification of a Lacrt ELP fusion protein

We designed the a gene encoding LV96 in the pET25b(+) vector resulting in the amino acid sequence shown in Table 1. V96 forms viscous coacervates with T_t below physiological temperatures of 37 °C [41] and thus was chosen as the ELP backbone for depot formation. LV96 was also used to generate free a Lacrt control protein utilizing selective cleavage of a thrombin cleavage site (Fig. 1A). In contrast to the previously reported intein system for Lacrt purification [14], LV96 fermentation yielded more than 40 mg/l using the inverse transition cycling purification approach followed by size exclusion chromatography at high purity (Fig. 1B). Interestingly, SDS-PAGE analysis of purified LV96 (Supplementary Fig. S1) suggested the spontaneous cleavage of ELP (V96) from the fusion construct, which yielded a combination of fusion protein and the ELP tag after purification. After optimization, a size exclusion chromatography was used to remove free ELP tags as a final purification step (Supplementary Fig. S1). Similar to previous reports [23], free Lacrt ran higher on SDS-PAGE than the expected M.W. of 12 kDa (Fig. 1B); however, its expected mass was confirmed by mass spectrometry (Table 1).

Optical density was used to characterize the phase behavior for all three constructs (Table 1), which revealed that only LV96 and V96 phase separate at physiological temperatures (Fig. 1C). The phase separation for LV96 was similarly confirmed using confocal microscopy and also dynamic light scattering (Supplementary Fig. S2) The LV96 phase transition curve at 25 μM (Fig. 1C) was consistent with the phase transition behavior of the parent V96 with an ~5 °C decrease. Further characterization of the concentration–temperature phase diagrams shows that LV96 is less dependent on concentration compared to V96 as fit by a log-linear regression line (Fig. 1D). Western blotting with antisera raised against the carboxy terminus of Lacrt (N-65) (Fig. 2A) further confirmed the successful production of Lacrt as a band that runs near 18 kDa [45]. To explore the stability of purified Lacrt, it was incubated for up to 2 days at physiological temperatures, which resulted in the appearance of major fragments (Fig. 2B), which were consistent with proteolysis at lysine residues (Table 2). At physiological temperatures, the cleavage half-life of disappearance for Lacrt is about one day (Fig. 2D); furthermore, this cleavage could be inhibited by a protease inhibitor cocktail (Supplementary Fig. S3). Despite this apparent biodegradation,

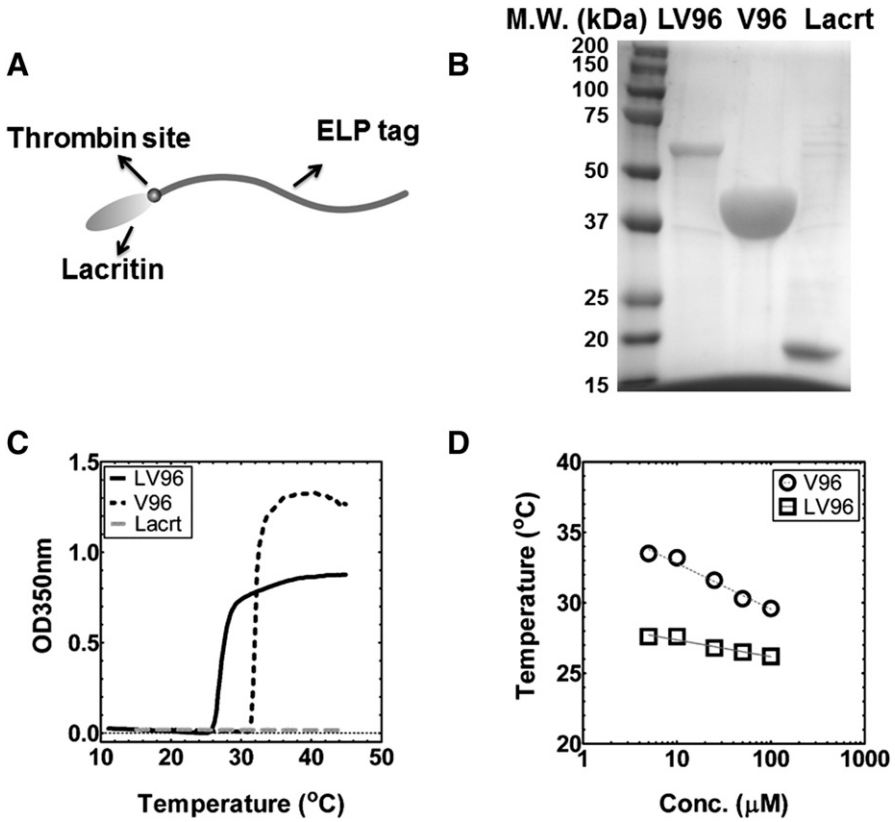

Fig. 1. Purification and thermal characterization of LV96. A) Cartoon of the LV96 fusion protein showing Lacrt at the N-terminus and an ELP tag at the C-terminus, with a thrombin recognition site between the two moieties. B) SDS-PAGE of purified LV96, ELP alone (V96) and free Lacrt. Gels were stained using $CuCl_2$. C) Representative optical density profiles for LV96, V96 and Lacrt at 25 μM as a function of temperature, which indicate a phase separation at 26.8 (LV96) and 31.6 °C (V96) respectively. Lacrt alone remains soluble, and does not increase optical density. D) A concentration temperature phase diagram was constructed. Best fit lines are indicated that follow Eq. (1) (Table 1).

by optimizing the purification strategy and maintaining proteins on ice, both Lacrt and LV96 were available at high purity and yields necessary for further study (Fig. 1B).

3.2. LV96 stimulates β-hexosaminidase secretion from primary rabbit LGACs

The concentration-dependent prosecretory activity of recombinant human Lacrt was first reported using freshly isolated rat lacrimal acinar cells with peroxidase as the marker of secretory activity [14]. Signaling was effective in cells exposed to 10 to 20 μM Lacrt as a coating solution and at 0.8 to 13 nM when presented as soluble Lacrt. The latter was confirmed in assays of several cultured human cell lines over a broad dose range [18]. Yet, Lacrt partially purified from monkey tears is apparently optimal at 1 μM. Further *in vivo* studies indicated that 0.8 to 8 μM Lacrt topically administered either as a single dose or chronically over two weeks elevated basal tearing of healthy New Zealand White adult female rabbits [46]. Rabbit LGACs do not secrete peroxidase; therefore, β-hexosaminidase secretion, an alternative secretory marker, was monitored from primary rabbit LGACs treated with a similar dose range for Lacrt or LV96 (Fig. 3). For all secretory studies, the small molecule carbachol (CCh) was used as a positive control. CCh acts on a broad spectrum of muscarinic and nicotinic acetylcholine GPCRs, including targets in the LG. This non-specificity makes CCh a poor therapeutic; however, as a positive control it can be used to assess maximal prosecretory capacity for the LG. With respect to no treatment or CCh, three treatment groups (Lacrt, LV96 and V96) were evaluated at four concentrations (0.1 to 20 μM) using a two-way ANOVA followed by Bonferroni post-hoc analysis (GraphPad Prism). Each treatment was performed in triplicate and three independent experiments were performed ($n = 9$). Compared to V96, the LV96 coacervate significantly stimulated secretion at a concentration of 10 μM ($p < 0.01$) and 20 μM ($p < 0.001$) while significant Lacrt-triggered stimulation was observed at 20 μM ($p < 0.05$) (Fig. 3B); the effects of either Lacrt or LV96 at 1 μM or 0.1 μM were not statistically significant. This data suggests that receptors exist on rabbit LGACs that respond to human Lacrt delivered by an ELP fusion.

In response to secretagogues, LGACs exocytose mature secretory vesicles containing tear proteins at their apical membranes for release into the acinar lumen, an event that involves F-actin remodeling around secretory vesicles at the luminal region [47]. Motivated to understand the cellular mechanisms of LGAC secretory activity in response to LV96, cellular morphology was tracked in live LGACs transduced with adenovirus Ad-LifeAct-RFP to observe changes in F-actin filament rearrangement at the apical and basolateral membranes during exocytosis (Fig. 3C). CCh acutely increased significant F-actin filament turnover and promoted transient actin coat assembly around apparent fusion intermediates within 10 min, as previously reported [47]. In contrast, LV96 exhibited a slower and sustained effect on F-actin remodeling, which triggered increased irregularity in the actin filaments around the lumen and formation of actin-coated structures beneath apical membranes (white arrows) after 26 min. No significant remodeling of actin filaments was observed in the V96 control group. This data confirms that LV96, even when incubated above its phase transition temperature, induces F-actin remodeling in rabbit LGACs, which is consistent with their secretion of β-hexosaminidase (Fig. 3B).

3.3. Fusion with V96 influences cellular uptake of exogenous Lacrt into LGACs

Secreted by LGAC, transported via ducts and deposited onto rapidly renewing ocular surface epithelia, Lacrt is thought to be preferentially

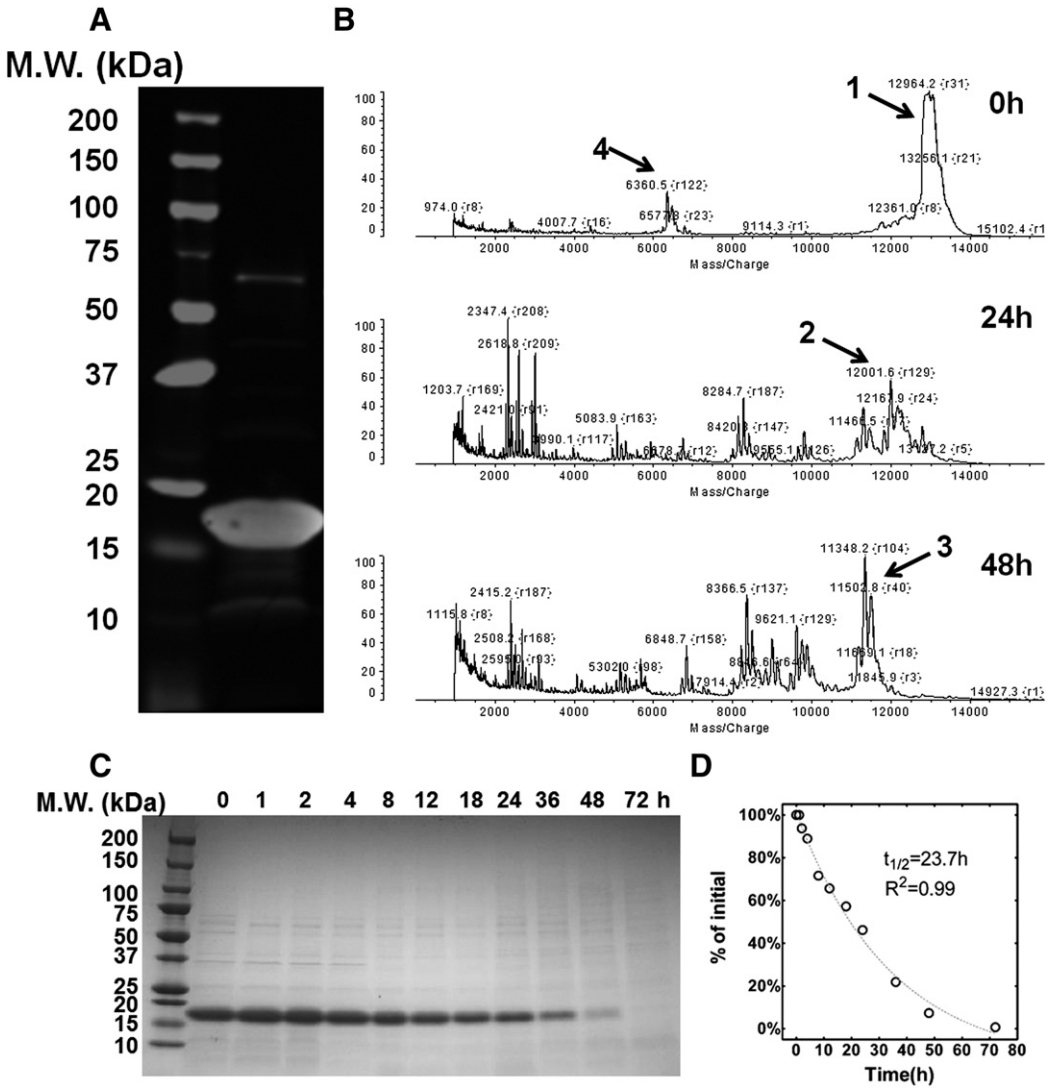

Fig. 2. Purified lacritin is susceptible to proteolysis of an unidentified origin. A) Western blot of purified Lacrt probed with an anti-Lacrt antibody (raised against Lacrt lacking 65 amino acids at the amino terminus) revealed a major band around 18 kDa, which is consistent with that observed previously for purified Lacrt. B) MALDI-TOF analysis of Lacrt revealed the appearance of major lower molecular weight fragments (Table 2) upon incubation at 37 °C in PBS. C) Time dependent disappearance of the purified Lacrt band by was tracked by SDS-PAGE stained with Coomassie blue. D) Lacrt disappearance was quantified and fitted to a single exponential decay model, which yielded a half-life of 23.7 h ($R^2 = 0.99$).

mitogenic or prosecretory for the cell types that it normally contacts during its glandular outward flow, such as the corneal, limbal and conjunctival epithelial cells, meibomian and LG epithelium, retina, and retinal pigmented epithelium/choroid [48]. Yet, no previous studies have captured the real-time binding and transport of Lacrt in live cells. Herein, live-cell confocal microscopy was used to document the time-dependent uptake of exogenous Lacrt and LV96 in rabbit LGACs (Fig. 4). Binding of native Lacrt to the basolateral membrane of LGAC was observed from 10 min of exposure (Fig. 4A). Significant levels of fluorescent puncta were observed in the cytosol after 30 min. Interestingly, there was an increase in accumulation in the apical lumen (white *), which suggests possible transcytosis of Lacrt from the basolateral to the apical membranes in LGACs. Similarly, LV96 was observed in intracellular puncta within LGACs, while LV96 treated cells showed lower levels of basolateral staining than Lacrt (Fig. 4B). The unmodified ELP, V96, did not undergo significant internalization into these

Table 2
Representative Lacritin cleavage sequences identified by MALDI-TOF.

Fragment	Amino acid sequence[a]	Exp. M.W.[b] [kDa]	Obs. M.W.[c] [kDa]
1	GEDASSDSTGADPAQEAGTSKPNEEISGPAEPASPPETTTTAQETSAAAVQGTAKVTSSRQELN PLKSIVEKSILLTEQALAKAGKGMHGGVPGGKQFIENGSEFAQKLLKKFSLLKPWAGLVPR	12.84	12.96
2	GEDASSDSTGADPAQEAGTSKPNEEISGPAEPASPPETTTTAQETSAAAVQGTAKVTSSRQELN PLKSIVEKSILLTEQALAKAGKGMHGGVPGGKQFIENGSEFAQKLLKKFSLLK	11.84/11.97	12.00
3	GEDASSDSTGADPAQEAGTSKPNEEISGPAEPASPPETTTTAQETSAAAVQGTAKVTSSRQELN PLKSIVEKSILLTEQALAKAGKGMHGGVPGGKQFIENGSEFAQKLLKK	11.25/11.38	11.35/11.47/11.50
4	PNEEISGPAEPASPPETTTTAQETSAAAVQGTAKVTSSRQELNPLKSIVEKSILLTEQALAK	6.42	6.36

[a] Underlined sequence: Syndecan-1 binding site.
[b] Expected M.W. (kDa) for fragments was calculated by DNAStar Lasergene Editseq.
[c] Observed M.W. (kDa) was measured by MALDI-TOF.

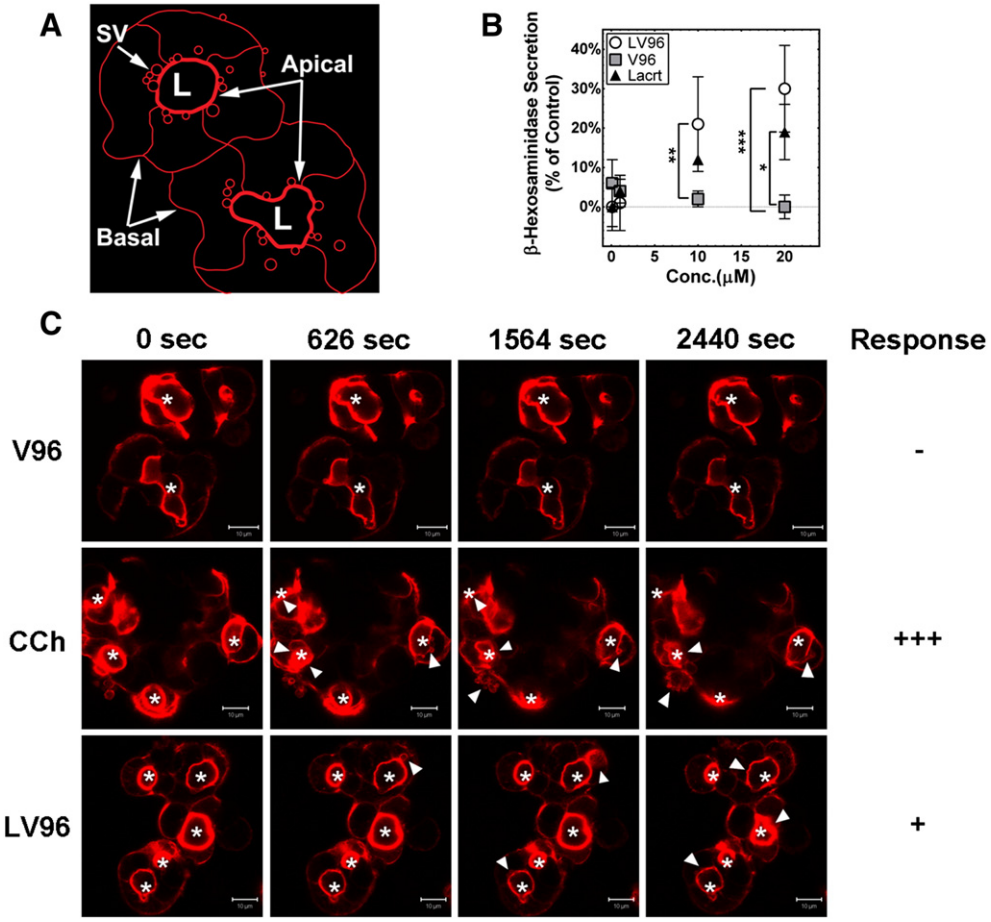

Fig. 3. Lacrt–ELP fusion proteins are prosecretory in LGACs. A) A cartoon depicts structure for *ex vivo* clusters of LGACs obtained from rabbits. These primary cultures form an apical lumen (L) that is bounded by a thick network of actin filaments. SV: secretory vesicles. B) Rabbit secretory vesicles (SV) release β-hexosaminidase in a dose dependent manner in response to secretagogues. The percentage of cellular secretion for each treatment (Eq. (2)) has been normalized to a positive control defined by CCh-stimulation, which is defined as 100%. LGACs were treated with 0.1 to 20 μM of LV96, Lacrt, V96, or no treatment for 1 h at 37 °C. 10 and 20 μM LV96 significantly enhanced secretion compared to the V96 group (**$p < 0.01$), and a similar effect was found with 20 μM Lacrt (*$p < 0.05$). Data were shown as mean ± S.D. and analyzed by ANOVA followed by Bonferroni's post-hoc test. C) Live-cell confocal microscopy was performed using LGACs labeled for F-actin (red). Actin-RFP is enriched beneath the apical membrane surrounding the lumen. Shortly after 10 min, increased irregularity of apical actin filaments and actin-coated secretory vesicle (SV) formation beneath the apical membrane (white arrows) were observed in CCh treated cells (100 μM). Similarly LV96 (20 μM) induced time-dependent actin remodeling after 26 min, which increased the irregularity of apical actin filaments and formation of secretory vesicles (white arrows). No significant remodeling of actin filaments was observed in a V96 treated control group. Apical lumen are indicated (white *). Scale bar: 10 μm.

cells (Fig. 4C). This fluorescent signal was quantified using image analysis and analyzed using a two-way ANOVA followed by Tukey's Post-hoc test (GraphPad Prism). At 10 min, both Lacrt and LV96 exhibited higher cellular uptake than V96. After 30 min, Lacrt underwent significantly higher uptake into LGACs (****$p < 0.0001$) than LV96 (Fig. 4D). After 2 h accumulation of Lacrt and LV96 in the acini was similar, although red puncta were slightly more prevalent in the Lacrt treated cells. The lower intracellular accumulation relative to free Lacrt is possibly caused by its phase separation, which could delay endocytosis [20].

3.4. LV96 stimulates tear secretion from non-obese diabetic (NOD) mice

To explore Lacrt's efficacy as a secretagogue in a murine model, Lacrt and LV96 were administered into non-obese diabetic (NOD) mice via intra-lacrimal injection and assessed for tear secretion (Fig. 5A). NOD mice have been established as a model for type-1 insulin-dependent diabetes mellitus [49] and one of the most utilized models for the study of DED symptomatic of Sjögren's syndrome [50–52], which is characterized by reduced production of aqueous tears [53] and autoimmune infiltration of LGs and salivary tissues [54]. Paradoxically, although Sjögren's syndrome is more prevalent in female patients, the 10–12 week male NOD mice feature earlier symptoms of autoimmune inflammation in LG, including severe lymphocytic infiltration (Fig. 5C), decreased production of lacrimal fluid, significant extracellular matrix degradation and increased expression of matrix metalloproteinases [55]. At 10–12 weeks of age female NOD mice maintain normal LG morphology (Fig. 5D); however, they do develop severe pathology in salivary tissues [54].

Using 10–12 week old NOD mice, four treatments were compared in an acute tear secretion study: CCh, V96, LV96 and Lacrt. Within each experiment, treatments were performed on three mice, and this experiment was repeated three times ($n = 9$). In each mouse, both LGs were treated. The tears were collected for 30 min from each eye and pooled to obtain the volume secreted per mouse. Results were then analyzed using a one-way ANOVA followed by Tukey's post-hoc test (GraphPad Prism). Immunohistochemistry revealed that intra-lacrimal injection of LV96 generates a local depot that is positive for human Lacrt immediately after injection (Fig. 5B). This depot was independently observed following intra-lacrimal injection into healthy mice, which revealed significantly more staining for LV96 than for free Lacrt (Supplementary Fig. S4). In normal mice, there was a small increase in tear volume for LV96 compared to the negative control V96; however, it was not significant (Supplementary Fig. S4). In contrast, for the NOD disease model LV96 and free Lacrt produced strong prosecretory activity in both

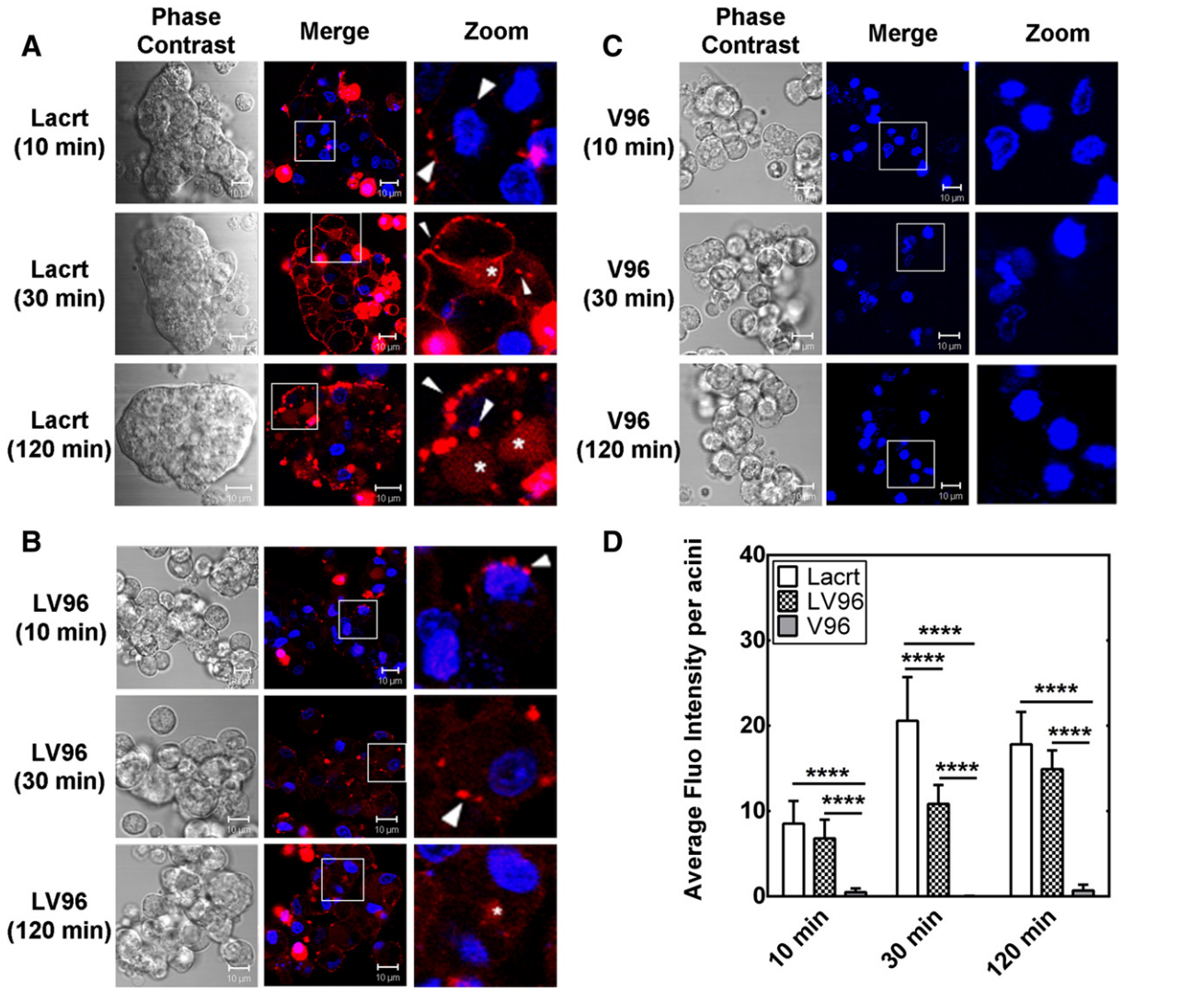

Fig. 4. Fusion with V96 influences uptake of exogenous Lacrt into LGACs. A) Time-dependent uptake of rhodamine-labeled Lacrt into rabbit LGACs was assessed by live-cell confocal microscopy. After 30 min, significant numbers of fluorescent puncta were detected in the cytosol proximal to the basolateral membrane (white arrow). More diffuse staining was observed within the lumen encircled by the apical membrane (white *), which suggest possible transcytosis. After 2 h, basolateral binding became less uniformly distributed. B) Time-dependent uptake of LV96 revealed a less intense labeling pattern at the basolateral membranes; however, there were significant levels of intracellular puncta (white arrows). Diffuse accumulation was detected in the apical lumen by 2 h (white *), although this effect was less pronounced than for free Lacrt. C) A negative control V96 did not show significant uptake into LGACs. Scale bar: 10 μm. D) Lacrt, LV96 and V96 intensity in LGACs was quantified at three time points. Both Lacrt and LV96 exhibited significantly (****$p < 0.0001$) higher uptake than V96. Lacrt entered LGACs to a greater extent than LV96, most obviously at 30 min (****$p < 0.0001$). Data were analyzed by a two-way ANOVA followed by Tukey's post-hoc test ($n = 9$).

males and females (Fig. 5E, F). Compared to CCh stimulation (100%), LV96's prosecretory effect was 40.9% in males and 50.0% in females, both significantly higher than V96 treatment ($p < 0.01$). Lacrt's efficacy was 29.6% in males and 42.9% in females. This data confirms the surprising *in vitro* finding (Fig. 3) that the phase separation of LV96 does not inhibit Lacrt-specific activity. Due to the acute nature of this assay, it was not expected that LV96 would produce a greater tear volume than free Lacrt.

To differentiate the *in vivo* potential of LV96 and free Lacrt, it was necessary to follow the LG up to a day after intra-lacrimal injection. In humans, the inferior palpebral lobe of the lacrimal gland is accessible for injection beneath the eyelid, which makes it a clinically relevant location for sustained release formulations. Unfortunately, in a murine model injection of the lacrimal gland requires surgical exposure of the injection site. This invasive procedure near the eye makes it challenging to attribute differences in basal tear production to the formulations. Therefore, to obtain evidence supporting the sustained retention of LV96, as compared to free Lacrt, the LG biodistributions of rhodamine labeled LV96 and Lacrt were assessed as a function of time at 2, 4, and 24 h after intra-LG injection (Fig. 6). Typically, eight slices (thickness: 8 μm/slice) of each sample with an interval of 80 μm were imaged to reflect the protein distribution in the whole LG. Each treatment and time point has been repeated in three independent LGs. Fluorescence intensity of the entire view or within a defined area was quantified using ImageJ. As shown in Figs. 6, 2 h after implantation LV96 remained in a deposit at the site of injection, which was more intense compared to Lacrt alone (Fig. 6A, B). This effect was quantified by image analysis (Fig. 6C). After 24 h LV96 coacervates remained obvious and showed little decrease in fluorescent intensity. In contrast, signal from free Lacrt was undetectable after 2 h (Fig. 6C). In addition, the depot maintains significant signal both at the center of the injection and also at a reference point taken 300 μm away (Fig. 6D, E). Between 4 and 24 h the intensity taken at the reference point changed minimally, which suggests the possibility that fluorescent LV96 is being released from the depot. In contrast, free Lacrt was not observed anywhere within the gland at 4 or 24 h.

4. Discussion

The eye is now a frequent target for development of new drugs, especially novel biological therapies [56] due to the increased numbers of

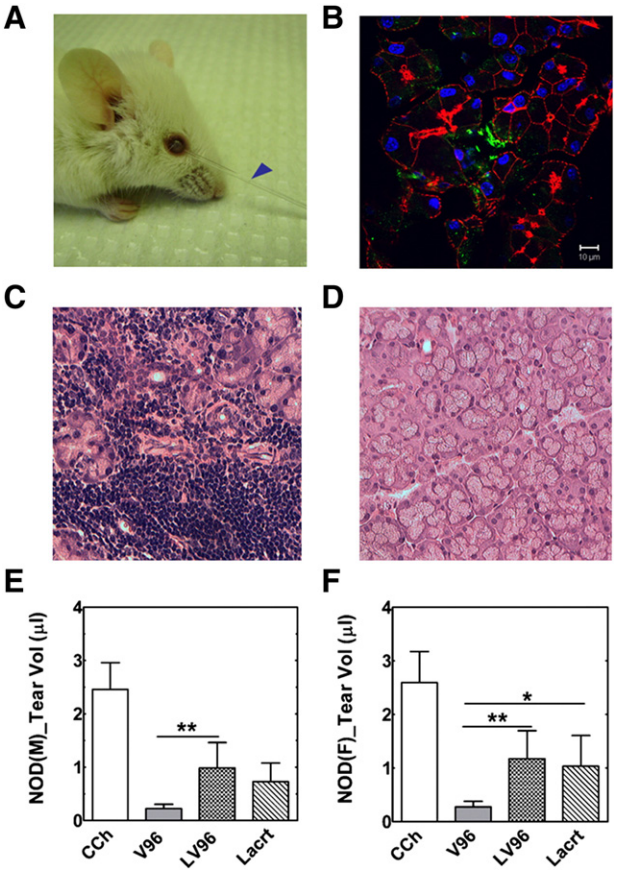

Fig. 5. Lacrt–ELP fusion proteins stimulate tear secretion in NOD mice. A) Representative pictures showing tear secretion stimulated by 100 μM LV96 (5 μl) after an intra-lacrimal injection in a male NOD mouse. Blue arrow: collected tear volume after 30 min. B) Lacrimal glands injected with LV96 were collected after infusion and visualized using immunofluorescence to identify Lacrt by an anti-C terminus Lacrt antibody. Green: anti-Lacrt antibody; Red: actin stained using Rho-phalloidin; Blue: nucleus stained by DAPI. Scale bar: 10 μm. C–D) Representative H&E staining images of NOD mouse lacrimal glands. C) Severe lymphocytic infiltration was observed in male NOD mice LG. D) Female NOD mice exhibited normal morphology. E–F) Tear volume quantification showing significant enhancement of tear secretion by LV96 and Lacrt compared to negative V96 controls ($^{**}p < 0.01$, $^{*}p < 0.05$, $n = 9$). Data are shown as mean ± S.D. and are compared by ANOVA followed by Tukey's Post Hoc Test. E) Male NOD mice; F) Female NOD mice.

patients with aging, ocular allergies and DED [57]. Local ocular delivery provides unique opportunities to enhance the therapeutic index of ophthalmic drugs by extending local residence time while minimizing off-target effects and dose frequency [58]. Over the past several decades, protein therapeutics have become highly successful because of their high target specificity, reduced interference with normal biological processes and minimal immune responses to human self-proteins [59]. The discovery of Lacrt offers a new therapeutic opportunity for DED and an alternative to conventional approaches [12]. Its basic structural features [12], prosecretory and mitogenic significance [14], as well as associated downstream signaling transduction mechanisms [18,20] have been gradually elucidated over the past decade.

As a proof of concept, this study characterizes a thermo-responsive Lacrt–ELP fusion protein for extended retention. The ELP V96 was fused to Lacrt to confer multiple functions: i) re-engineer Lacrt with the ability to form an intra-lacrimal depot at physiological temperatures; ii) to maintain Lacrt-mediated cell signaling. Together, these properties support the further development of Lacrt or other biologicals into sustained-release biopharmaceuticals for ophthalmology. The transition temperature (Fig. 1C, D) and thermo-responsive assembly of LV96 (Supplementary Fig. S2) supports the hypothesis that Lacrt fused to an ELP exhibits similar phase separation and self-assembly properties relative to the parent ELP. Significantly enhanced β-hexosaminidase secretion and actin remodeling from primary rabbit LGACs (Fig. 3) and increased tear secretion from both male and female NOD mice (Fig. 5) corroborated the prosecretory activity of LV96, even above its phase transition temperature. Despite having similar prosecretory activity, cellular internalization studies revealed a distinctly slower pattern of uptake for LV96 coacervates compared to free Lacrt (Fig. 4). Based on this assessment, the microbiodistribution of LV96 following intra-lacrimal administration was characterized via indirect immunofluorescence (Fig. 5B, Supplementary Fig. S4) and by covalent labeling (Fig. 6). These data definitively show that Lacrt fused to an ELP maintains significantly more fluorescence than free Lacrt at all times post-injection. In other disease models, it was recently shown that phase separation of ELPs in a tumor slowed the local half-life of clearance by more than an order of magnitude [60]. Similarly, extended control over blood glucose level was observed using a depot of a therapeutic ELP [61]. Thus, the ocular data presented here support the hypothesis that Lacrt fused to an ELP remains prosecretory both *in vitro* and *in vivo*; furthermore, its ability to form a local depot is consistent with previous literature in other disease models.

Interestingly, Lacrt demonstrated a susceptibility to protease degradation based on MALDI-TOF analysis (Fig. 2B) and time-dependent analysis of degradation by SDS-PAGE (Fig. 2C), which together suggest that native Lacrt has a cleavage half-life of about one day at 37 °C (Fig. 2D). The biodegradation of Lacrt was consistent with the generation of peptides that were cleaved between lysine residues found in human Lacrt (Table 2). Trypsin-like serine proteases cleave peptide bonds next to lysine or arginine residues, with serine performing the nucleophilic attack and negatively charged aspartic acid controlling the specificity [62–64]. *In silico* analysis by the Protease Specificity Prediction Server suggested Lacrt's serine protease sensitivity liberates the C-terminal amphipathic α-helix intact for downstream co-receptor binding to syndecan-1 (Table 2) [65]. Recent reports suggest that this proteolysis releases an α-helical carboxy terminal peptide from Lacrt that displays bactericidal activity, which may represent an innate defensive immunity on the ocular surface [66]. The cleavage may be regulated by serine proteases, as specific protease inhibitors (chymostatin, leupeptin) or boiling were reported to inhibit proteolysis. This report confirms that this proteolytic activity can be inhibited by a standard cocktail of protease inhibitors (Supplemental Fig. S3). This proteolysis was also observed for LV96 during purification (Supplemental Fig. S1). To maintain a single band by SDS-PAGE for purified LV96 (Fig. 1B), sample aliquots were frozen after purification and thawed on ice. Future studies are required to determine the source of this proteolysis, which may be attributed to either: i) trace proteases from bacterial fermentation; or ii) the possibility that Lacrt exhibits autolytic activation similar to trypsin [67]. In addition, the impact of glycosylation or other regulatory mechanisms to control the cleavage of native Lacrt remain to be determined.

Previously, Lacrt's *in vivo* prosecretory activity has been reported using New Zealand white rabbits via topical administration [16]. Recently, Vijmasi and coworkers tested Aire-knockout mice and proved that a long-term topical Lacrt treatment promoted tear secretion, restored ocular surface integrity, and reduced CD4+ T cell infiltration of the LG [17]. Aire-knockout mice are an aqueous-deficient dry eye mouse model that is deficient in the autoimmune regulator (Aire) gene. This model was derived from the non-obese diabetic (NOD) and Balb/c mice background. Here we found that the NOD mouse strain also was highly responsive to the effect of exogenous Lacrt (Fig. 5); furthermore these effects were significantly greater than those observed in a normal mouse (Supplementary Fig. S4). The disparities associated with the NOD disease mice and the C57BL/6 healthy mouse models suggest that features of aqueous tear deficiency may sensitize the diseased LG to therapy with Lacrt. Although the molecular mechanism for Lacrt's prosecretory signaling remains under study, its carboxy-terminus is

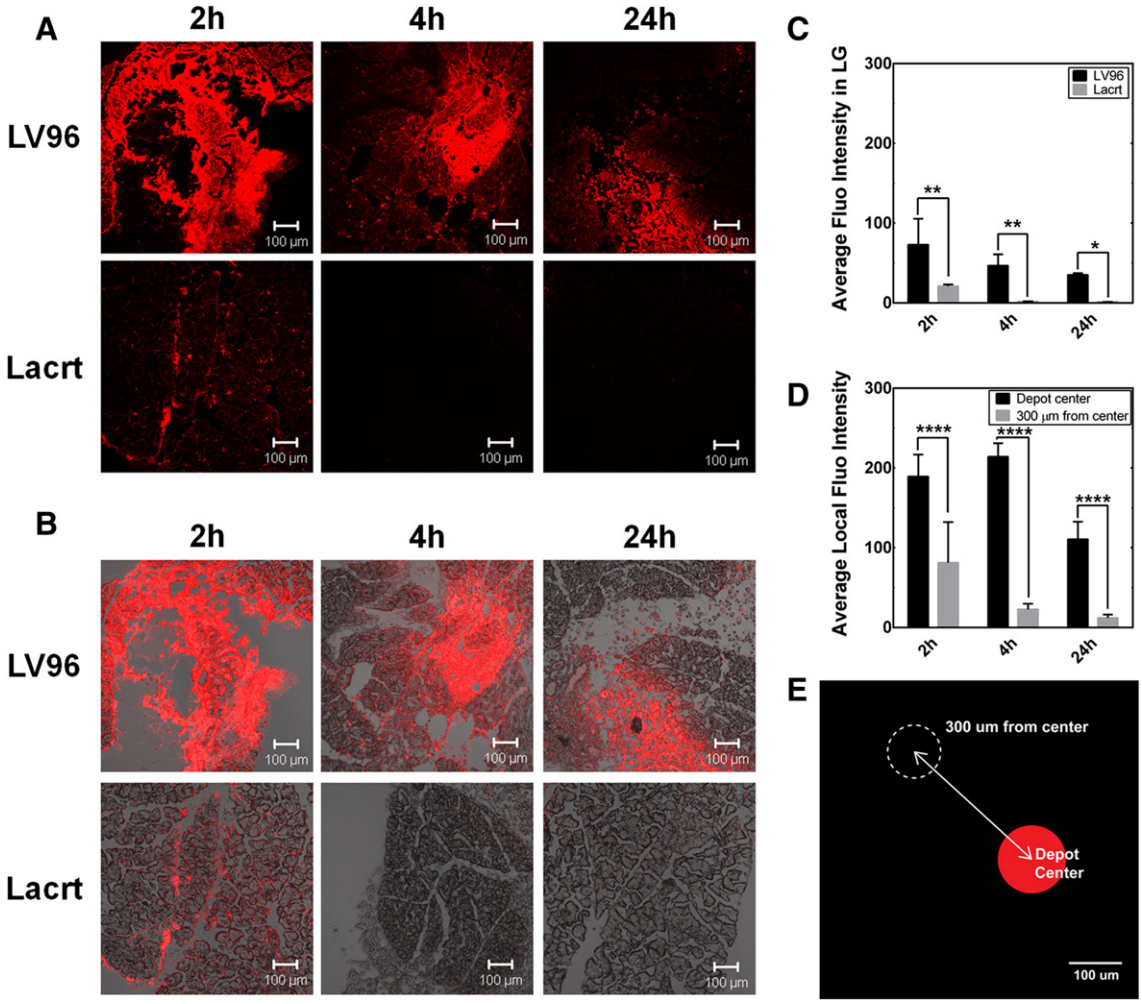

Fig. 6. Intra-lacrimal injection of Lacrt–ELP fusion protein produces a depot. A, B) Representative confocal images showing exogenous rhodamine-labeled LV96, which forms a depot in the LG of female C57BL/6 mice. LV96 was strongly retained over the 24 h time course, while free Lacrt was not observed after just 4 h. A) Rhodamine signal alone. B) Merged combinations of phase contrast and rhodamine signal. C) Quantification of average fluorescence intensity in the section of LG centered on the injection, which shows that LV96 is retained longer than free Lacrt (*$p < 0.05$, **$p < 0.01$). D & E) After injection, depots of LV96 maintained a lower concentration (**** < 0.0001) at a distance of 300 μm from the depot center; however, this fluorescence was greater than that detected either in surrounding or untreated acini. Scale bar: 100 μm.

known to bind specifically to heparanase activated syndecan-1 [20]. Vijmasi and coworkers hypothesized that via topical administration, Lacrt may play a functional role in maintaining corneal innervation during homeostasis, interrupting or mitigating the inflammatory cycle, and thus protecting the LG from focal infiltration of auto-antigen primed CD4+ T cells [17]. This report provides the first *in vivo* evidence of Lacrt's prosecretory effect upon direct interaction with the LG. Further investigations regarding syndecan-1 and heparanase expression level in different mice LGs, Lacrt's affinity towards receptors expressed in the LG, its neuronal stimulation mechanism and differences among various mice strains will be necessary to better understand the mechanism of Lacrt therapies.

Exhibiting prosecretory, mitogenic, cytoprotective and bactericidal functions, Lacrt may recruit different signaling pathways for each of these activities. For example, previous reports have explored intracellular Ca^{2+} changes in response to Lacrt, which is readily evident in the corneal epithelium [39]. Being an important early messenger in signal transduction cascades, Ca^{2+} can indicate different signals by changing its transient cytosolic oscillation frequency [68]. In the LG acinar cells, cholinergic agonists stimulate protein secretion by binding to receptors in the basolateral membrane of secretory cells and activating phospholipase C to break down phosphatidylinositol bisphosphate into 1,4,5-inositol trisphosphate (1,4,5-IP3) and diacylglycerol (DAG). 1,4,5-IP3 causes intracellular release of Ca^{2+}, which works together with calmodulin and further activates specific protein kinases that may be involved in secretion [69]. Interestingly, of all the treatment groups tested herein, only carbachol (CCh) triggered cytoplasmic Ca^{2+} concentration change in LGACs (Supplementary Fig. S5), while no significant signals were observed in EGF, Lacrt or LV96 treatment groups. Consistent with this observation, Sanghi and coworkers discussed a similar loss of Ca^{2+} activation in Lacrt's prosecretory activity pathway [14]. Although Lacrt and LV96 only exhibited 10–30% of the control CCh response in the β-hexosaminidase secretion assay (Fig. 3B), these findings are consistent with the possibility that Lacrt may recruit alternative pathways for its prosecretory function. While CCh acts on a broad spectrum of muscarinic acetylcholine G-protein coupled receptors (GPCRs) as well as nicotinic acetylcholine receptors (ligand-gated ion channels), Lacrt's signaling pathway may be more specific.

This specificity may be due to its involvement with deglycanated syndecan-1, which enables it to act on an as of yet unidentified GPCR [12]. The carboxy-terminal amphipathic α-helix of Lacrt has been reported to associate with co-receptor syndecan-1, which thus regulates functional specificity [20] and maintains corneal epithelium homeostasis [19]. New data suggested that the same region undergoes proteolytic processing and demonstrates crucial bactericidal activity in tears [66]. Similar to our recent reports in SV40-transduced human

corneal epithelial cells (HCE-Ts) [39], Lacrt triggers a cascade of mitogenic events involving Gαi or Gαo–PKCα-PLC–Ca^{2+}–calcineurin–NFATC1 and Gαi or Gαo–PKCα–PLC–phospholipase D (PLD)–mTOR pathways [18].

The concept of a 'reservoir drug' [70] is intended to tackle the problem of inefficient target delivery and rapid payload clearance. By modulating the precise location and residence time of the therapeutic agent, side effects (such as those produced by CCh) can be reduced and efficacy may be enhanced [71]. ELPs have shown promise as reservoir scaffolds [30,34], and now provide an emerging alternative to PLGA [72] or catechol-based gels [73]. Prior to this study, it was unclear if polymer modification and phase separation would sterically hinder Lacrt and thus impair its activity. Thus, we have now verified both *in vitro* and *in vivo* that LV96 is equivalent in potency to free Lacrt. Moreover, the phase separation of the V96 tag slows cellular uptake and promotes retention in the LG. Based on this report, and of those noted above for free Lacrt, we can propose a mechanism of action for an LV96 drug depot (Supplementary Fig. S6); however, additional studies will be required to confirm this model. Further study of Lacrt ELP fusions are require required that explore the local and systemic pharmacokinetics as well as the molecular mechanisms of Lacrt release, receptor-mediated binding, and cellular signaling involved with tear secretion.

5. Conclusion

Achieving sustained delivery of therapeutic proteins is one of the major challenges of ophthalmology. In pursuing this goal, ELPs were fused with the model dry eye disease biopharmaceutical, Lacrt. Lacrt–ELP fusion proteins demonstrated thermo-responsive phase separation, similar to that exhibited by the parent ELPs. They also gained the prosecretory activity of human Lacrt. ELP modification influenced cell uptake speed, enhanced local retention time in the LG, and provided Lacrt-mediated signaling. If successful, this approach may be useful to deliver a variety of proteins to ocular targets.

Acknowledgments

This study is supported by the USAMRMC/TATRC grant W81XWH1210538, NIH EY011386, and the USC Whittier foundation. The authors appreciate the excellent technical support of rabbit lacrimal gland acinar cells (LGACs) preparation by Hua Pei.

Appendix A. Supplementary data

Supplementary data to this article can be found online at http://dx.doi.org/10.1016/j.jconrel.2014.11.016.

References

[1] D.A. Dartt, Neural regulation of lacrimal gland secretory processes: relevance in dry eye diseases, Prog. Retin. Eye Res. 28 (2009) 155–177.
[2] G.W. Laurie, L.A. Olsakovsky, B.P. Conway, R.L. McKown, K. Kitagawa, J.J. Nichols, Dry eye and designer ophthalmics, Optom. Vis. Sci. 85 (2008) 643–652.
[3] N.J. Friedman, Impact of dry eye disease and treatment on quality of life, Curr. Opin. Ophthalmol. 21 (2010) 310–316.
[4] M.E. Stern, R.W. Beuerman, R.I. Fox, J.P. Gao, A.K. Mircheff, S.C. Pflugfelder, The pathology of dry eye: the interaction between the ocular surface and lacrimal glands, Cornea 17 (1998) 584–589.
[5] M.A. Javadi, S. Feizi, Dry eye syndrome, J. Ophthalmic Vis. Res. 6 (2011) 192–198.
[6] J. Qiao, X. Yan, Emerging treatment options for meibomian gland dysfunction, Clin. Ophthalmol. 7 (2013) 1797–1803.
[7] T. Kojima, Y. Matsumoto, O.M. Ibrahim, T.H. Wakamatsu, M. Dogru, K. Tsubota, Evaluation of a thermosensitive atelocollagen punctal plug treatment for dry eye disease, Am J. Ophthalmol. 157 (2014) 311–317 (e311).
[8] H.E. Kaufman, T.L. Steinemann, E. Lehman, H.W. Thompson, E.D. Varnell, J.T. Jacob-LaBarre, B.M. Gebhardt, Collagen-based drug delivery and artificial tears, J. Ocul. Pharmacol. 10 (1994) 17–27.
[9] R. Lu, R. Huang, K. Li, X. Zhang, H. Yang, Y. Quan, Q. Li, The influence of benign essential blepharospasm on dry eye disease and ocular inflammation, Am J. Ophthalmol. 157 (2014) 591–597 (e591–592).
[10] Y. Wei, N. Gadaria-Rathod, S. Epstein, P. Asbell, Tear cytokine profile as a noninvasive biomarker of inflammation for ocular surface diseases: standard operating procedures, Invest. Ophthalmol. Vis. Sci. 54 (2013) 8327–8336.
[11] E.K. Akpek, K.B. Lindsley, R.S. Adyanthaya, R. Swamy, A.N. Baer, P.J. McDonnell, Treatment of Sjogren's syndrome-associated dry eye an evidence-based review, Ophthalmology 118 (2011) 1242–1252.
[12] R.L. McKown, N. Wang, R.W. Raab, R. Karnati, Y. Zhang, P.B. Williams, G.W. Laurie, Lacritin and other new proteins of the lacrimal functional unit, Exp. Eye Res. 88 (2009) 848–858.
[13] R. Karnati, D.E. Laurie, G.W. Laurie, Lacritin and the tear proteome as natural replacement therapy for dry eye, Exp. Eye Res. 117 (2013) 39–52.
[14] S. Sanghi, R. Kumar, A. Lumsden, D. Dickinson, V. Klepeis, V. Trinkaus-Randall, H.F. Frierson Jr., G.W. Laurie, cDNA and genomic cloning of lacritin, a novel secretion enhancing factor from the human lacrimal gland, J. Mol. Biol. 310 (2001) 127–139.
[15] A. Fujii, A. Morimoto-Tochigi, R.D. Walkup, T.R. Shearer, M. Azuma, Lacritin-induced secretion of tear proteins from cultured monkey lacrimal acinar cells, Invest. Ophthalmol. Vis. Sci. 54 (2013) 2533–2540.
[16] S. Samudre, F.A. Lattanzio Jr., V. Lossen, A. Hosseini, J.D. Sheppard Jr., R.L. McKown, G.W. Laurie, P.B. Williams, Lacritin, a novel human tear glycoprotein, promotes sustained basal tearing and is well tolerated, Invest. Ophthalmol. Vis. Sci. 52 (2011) 6265–6270.
[17] T. Vijmasi, F.Y. Chen, S. Balasubbu, M. Gallup, R.L. McKown, G.W. Laurie, N.A. McNamara, Topical administration of lacritin is a novel therapy for aqueous-deficient dry eye disease, Invest. Ophthalmol. Vis. Sci. 55 (8) (2014 Jul 17) 5401–5409.
[18] J. Wang, N. Wang, J. Xie, S.C. Walton, R.L. McKown, R.W. Raab, P. Ma, S.L. Beck, G.L. Coffman, I.M. Hussaini, G.W. Laurie, Restricted epithelial proliferation by lacritin via PKCalpha-dependent NFAT and mTOR pathways, J. Cell Biol. 174 (2006) 689–700.
[19] N. Wang, K. Zimmerman, R.W. Raab, R.L. McKown, C.M. Hutnik, V. Talla, M.F.t. Tyler, J.K. Lee, G.W. Laurie, Lacritin rescues stressed epithelia via rapid forkhead box O3 (FOXO3)-associated autophagy that restores metabolism, J. Biol. Chem. 288 (2013) 18146–18161.
[20] P. Ma, S.L. Beck, R.W. Raab, R.L. McKown, G.L. Coffman, A. Utani, W.J. Chirico, A.C. Rapraeger, G.W. Laurie, Heparanase deglycanation of syndecan-1 is required for binding of the epithelial-restricted prosecretory mitogen lacritin, J. Cell Biol. 174 (2006) 1097–1106.
[21] Y. Zhang, N. Wang, R.W. Raab, R.L. McKown, J.A. Irwin, I. Kwon, T.H. van Kuppevelt, G.W. Laurie, Targeting of heparanase-modified syndecan-1 by prosecretory mitogen lacritin requires conserved core GAGAL plus heparan and chondroitin sulfate as a novel hybrid binding site that enhances selectivity, J. Biol. Chem. 288 (2013) 12090–12101.
[22] V.F. Velez, J.A. Romano, R.L. McKown, K. Green, L.W. Zhang, R.W. Raab, D.S. Ryan, C.M.L. Hutnik, H.F. Frierson, G.W. Laurie, Tissue transglutaminase is a negative regulator of monomeric lacritin bioactivity, Invest. Ophthalmol. Vis. Sci. 54 (2013) 2123–2132.
[23] P. Ma, N. Wang, R.L. McKown, R.W. Raab, G.W. Laurie, Focus on molecules: lacritin, Exp. Eye Res. 86 (2008) 457–458.
[24] S.V. Aluru, S. Agarwal, B. Srinivasan, G.K. Iyer, S.M. Rajappa, U. Tatu, P. Padmanabhan, N. Subramanian, A. Narayanasamy, Lacrimal proline rich 4 (LPRR4) protein in the tear fluid is a potential biomarker of dry eye syndrome, PLoS One 7 (2012).
[25] H. Rosen, T. Abribat, The rise and rise of drug delivery, Nat. Rev. Drug Discov. 4 (2005) 381–385.
[26] J.A. Hubbell, A. Chilkoti, Chemistry. Nanomaterials for drug delivery, Science 337 (2012) 303–305.
[27] J. Dhandhukia, I. Weitzhandler, W. Wang, J.A. MacKay, Switchable elastin-like polypeptides that respond to chemical inducers of dimerization, Biomacromolecules 14 (2013) 976–985.
[28] S.R. Aluri, P. Shi, J.A. Gustafson, W. Wang, Y.A. Lin, H. Cui, S. Liu, P.S. Conti, Z. Li, P. Hu, A.L. Epstein, J.A. MacKay, A hybrid protein–polymer nanoworm potentiates apoptosis better than a monoclonal antibody, ACS Nano 8 (2014) 2064–2076.
[29] P. Shi, S. Aluri, Y.A. Lin, M. Shah, M. Edman, J. Dhandhukia, H. Cui, J.A. Mackay, Elastin-based protein polymer nanoparticles carrying drug at both corona and core suppress tumor growth in vivo, J. Control. Release 171 (3) (2013 Nov 10) 330–338.
[30] M. Amiram, K.M. Luginbuhl, X. Li, M.N. Feinglos, A. Chilkoti, Injectable protease-operated depots of glucagon-like peptide-1 provide extended and tunable glucose control, Proc. Natl. Acad. Sci. U. S. A. 110 (2013) 2792–2797.
[31] D.E. Meyer, A. Chilkoti, Purification of recombinant proteins by fusion with thermally-responsive polypeptides, Nat. Biotechnol. 17 (1999) 1112–1115.
[32] E. Wang, M.S. Desai, S.W. Lee, Light-controlled graphene–elastin composite hydrogel actuators, Nano Lett. 13 (2013) 2826–2830.
[33] D.L. Nettles, A. Chilkoti, L.A. Setton, Applications of elastin-like polypeptides in tissue engineering, Adv. Drug Deliv. Rev. 62 (2010) 1479–1485.
[34] P. Koria, H. Yagi, Y. Kitagawa, Z. Megeed, Y. Nahmias, R. Sheridan, M.L. Yarmush, Self-assembling elastin-like peptides growth factor chimeric nanoparticles for the treatment of chronic wounds, Proc. Natl. Acad. Sci. U. S. A. 108 (2011) 1034–1039.
[35] D.J. Callahan, W. Liu, X. Li, M.R. Dreher, W. Hassouneh, M. Kim, P. Marszalek, A. Chilkoti, Triple stimulus-responsive polypeptide nanoparticles that enhance intratumoral spatial distribution, Nano Lett. 12 (2012) 2165–2170.
[36] J.A. MacKay, M. Chen, J.R. McDaniel, W. Liu, A.J. Simnick, A. Chilkoti, Self-assembling chimeric polypeptide–doxorubicin conjugate nanoparticles that abolish tumours after a single injection, Nat. Mater. 8 (2009) 993–999.
[37] M. Shah, M.C. Edman, S.R. Janga, P. Shi, J. Dhandhukia, S. Liu, S.G. Louie, K. Rodgers, J.A. Mackay, S.F. Hamm-Alvarez, A rapamycin-binding protein polymer nanoparticle

shows potent therapeutic activity in suppressing autoimmune dacryoadenitis in a mouse model of Sjogren's syndrome, J. Control. Release 171 (3) (2013 Nov 10) 269–279.
[38] W. Wang, P.G. Sreekumar, V. Valluripalli, P. Shi, J. Wang, Y.A. Lin, H. Cui, R. Kannan, D.R. Hinton, J.A. Mackay, Protein polymer nanoparticles engineered as chaperones protect against apoptosis in human retinal pigment epithelial cells, J. Control. Release (2014).
[39] W. Wang, J. Despanie, P. Shi, M.C. Edman-Woolcott, Y.-A. Lin, H. Cui, J. Heur, E. Fini, S.F. Hamm-Alvarez, J.A. MacKay, Lacritin-mediated regeneration of the corneal epithelia by protein polymer nanoparticles, J. Mater. Chem. B 2 (2014) 8131–8141.
[40] J.R. McDaniel, J.A. Mackay, F.G. Quiroz, A. Chilkoti, Recursive directional ligation by plasmid reconstruction allows rapid and seamless cloning of oligomeric genes, Biomacromolecules 11 (2010) 944–952.
[41] S.M. Janib, M. Pastuszka, S. Aluri, Z. Folchman-Wagner, P.Y. Hsueh, P. Shi, A. Yi, H. Cui, J.A. Mackay, A quantitative recipe for engineering protein polymer nanoparticles, Polym. Chem. 5 (2014) 1614–1625.
[42] D.E. Laurie, R.K. Splan, K. Green, K.M. Still, R.L. McKown, G.W. Laurie, Detection of prosecretory mitogen lacritin in nonprimate tears primarily as a C-terminal-like fragment, Invest. Ophthalmol. Vis. Sci. 53 (2012) 6130–6136.
[43] S.R. da Costa, F.A. Yarber, L. Zhang, M. Sonee, S.F. Hamm-Alvarez, Microtubules facilitate the stimulated secretion of beta-hexosaminidase in lacrimal acinar cells, J. Cell Sci. 111 (Pt 9) (1998) 1267–1276.
[44] L. Chiang, J. Ngo, J.E. Schechter, S. Karvar, T. Tolmachova, M.C. Seabra, A.N. Hume, S.F. Hamm-Alvarez, Rab27b regulates exocytosis of secretory vesicles in acinar epithelial cells from the lacrimal gland, Am. J. Physiol. Cell Physiol. 301 (2011) C507–C521.
[45] K. Seifert, N.C. Gandia, J.K. Wilburn, K.S. Bower, R.K. Sia, D.S. Ryan, M.L. Deaton, K.M. Still, V.C. Vassilev, G.W. Laurie, R.L. McKown, Tear lacritin levels by age, sex, and time of day in healthy adults, Invest. Ophthalmol. Vis. Sci. 53 (2012) 6610–6616.
[46] D. Kurzbach, W. Hassouneh, J.R. McDaniel, E.A. Jaumann, A. Chilkoti, D. Hinderberger, Hydration layer coupling and cooperativity in phase behavior of stimulus responsive peptide polymers, J. Am. Chem. Soc. 135 (2013) 11299–11308.
[47] G.V. Jerdeva, K. Wu, F.A. Yarber, C.J. Rhodes, D. Kalman, J.E. Schechter, S.F. Hamm-Alvarez, Actin and non-muscle myosin II facilitate apical exocytosis of tear proteins in rabbit lacrimal acinar epithelial cells, J. Cell Sci. 118 (2005) 4797–4812.
[48] Y. Zhang, R.L. McKown, R.W. Raab, A.C. Rapraeger, G.W. Laurie, Focus on molecules: syndecan-1, Exp. Eye Res. 93 (2011) 329–330.
[49] Y. Tochino, The NOD mouse as a model of type I diabetes, Crit. Rev. Immunol. 8 (1987) 49–81.
[50] C.P. Robinson, S. Yamachika, C.E. Alford, C. Cooper, E.L. Pichardo, N. Shah, A.B. Peck, M.G. Humphreys-Beher, Elevated levels of cysteine protease activity in saliva and salivary glands of the nonobese diabetic (NOD) mouse model for Sjogren syndrome, Proc. Natl. Acad. Sci. U. S. A. 94 (1997) 5767–5771.
[51] R.E. Hunger, S. Muller, J.A. Laissue, M.W. Hess, C. Carnaud, I. Garcia, C. Mueller, Inhibition of submandibular and lacrimal gland infiltration in nonobese diabetic mice by transgenic expression of soluble TNF-receptor p55, J. Clin. Invest. 98 (1996) 954–961.
[52] P.A. Moore, D.I. Bounous, R.L. Kaswan, M.G. Humphreys-Beher, Histologic examination of the NOD-mouse lacrimal glands, a potential model for idiopathic autoimmune dacryoadenitis in Sjogren's syndrome, Lab. Anim. Sci. 46 (1996) 125–128.
[53] M.G. Humphreys-Beher, Y. Hu, Y. Nakagawa, P.L. Wang, K.R. Purushotham, Utilization of the non-obese diabetic (NOD) mouse as an animal model for the study of secondary Sjogren's syndrome, Adv. Exp. Med. Biol. 350 (1994) 631–636.
[54] I. Toda, B.D. Sullivan, E.M. Rocha, L.A. Da Silveira, L.A. Wickham, D.A. Sullivan, Impact of gender on exocrine gland inflammation in mouse models of Sjogren's syndrome, Exp. Eye Res. 69 (1999) 355–366.
[55] K. Schenke-Layland, J. Xie, M. Magnusson, E. Angelis, X. Li, K. Wu, D.P. Reinhardt, W.R. Maclellan, S.F. Hamm-Alvarez, Lymphocytic infiltration leads to degradation of lacrimal gland extracellular matrix structures in NOD mice exhibiting a Sjogren's syndrome-like exocrinopathy, Exp. Eye Res. 90 (2010) 223–237.
[56] K. Garber, Biotech in a blink, Nat. Biotechnol. 28 (2010) 311–314.
[57] A.F. Clark, T. Yorio, Ophthalmic drug discovery, Nat. Rev. Drug Discov. 2 (2003) 448–459.
[58] G.D. Novack, Ophthalmic drug delivery: development and regulatory considerations, Clin. Pharmacol. Ther. 85 (2009) 539–543.
[59] B. Leader, Q.J. Baca, D.E. Golan, Protein therapeutics: a summary and pharmacological classification, Nat. Rev. Drug Discov. 7 (2008) 21–39.
[60] W. Liu, J.A. MacKay, M.R. Dreher, M. Chen, J.R. McDaniel, A.J. Simnick, D.J. Callahan, M.R. Zalutsky, A. Chilkoti, Injectable intratumoral depot of thermally responsive polypeptide–radionuclide conjugates delays tumor progression in a mouse model, J. Control. Release 144 (2010) 2–9.
[61] M. Amiram, K.M. Luginbuhl, X. Li, M.N. Feinglos, A. Chilkoti, A depot-forming glucagon-like peptide-1 fusion protein reduces blood glucose for five days with a single injection, J. Control. Release 172 (2013) 144–151.
[62] L. Hedstrom, Serine protease mechanism and specificity, Chem. Rev. 102 (2002) 4501–4524.
[63] L.B. Evnin, J.R. Vasquez, C.S. Craik, Substrate specificity of trypsin investigated by using a genetic selection, Proc. Natl. Acad. Sci. U. S. A. 87 (1990) 6659–6663.
[64] L. Polgar, The catalytic triad of serine peptidases, Cell Mol. Life Sci. 62 (2005) 2161–2172.
[65] J. Song, H. Tan, A.J. Perry, T. Akutsu, G.I. Webb, J.C. Whisstock, R.N. Pike, PROSPER: an integrated feature-based tool for predicting protease substrate cleavage sites, PLoS One 7 (2012) e50300.
[66] R.L. McKown, E.V. Coleman Frazier, K.K. Zadrozny, A.M. Deleault, R.W. Raab, D.S. Ryan, R.K. Sia, J.K. Lee, G.W. Laurie, A cleavage potentiated fragment of tear lacritin is bactericidal, J. Biol. Chem. 289 (32) (2014 Aug 8) 22172–22182.
[67] M.M. Vestling, C.M. Murphy, C. Fenselau, Recognition of trypsin autolysis products by high-performance liquid chromatography and mass spectrometry, Anal. Chem. 62 (1990) 2391–2394.
[68] D. Kraus, I. Kaiserman, J. Frucht-Pery, R. Rahamimoff, Calcium—an "all-round player" in the cornea, Isr. Med. Assoc. J. 3 (2001) 269–274.
[69] D.A. Dartt, Signal transduction and control of lacrimal gland protein secretion: a review, Curr. Eye Res. 8 (1989) 619–636.
[70] L. Setton, Polymer therapeutics: reservoir drugs, Nat. Mater. 7 (2008) 172–174.
[71] R. Langer, Drug delivery. Drugs on target, Science 293 (2001) 58–59.
[72] M. Parent, C. Nouvel, M. Koerber, A. Sapin, P. Maincent, A. Boudier, PLGA in situ implants formed by phase inversion: critical physicochemical parameters to modulate drug release, J. Control. Release 172 (2013) 292–304.
[73] C.J. Kastrup, M. Nahrendorf, J.L. Figueiredo, H. Lee, S. Kambhampati, T. Lee, S.W. Cho, R. Gorbatov, Y. Iwamoto, T.T. Dang, P. Dutta, J.H. Yeon, H. Cheng, C.D. Pritchard, A.J. Vegas, C.D. Siegel, S. MacDougall, M. Okonkwo, A. Thai, J.R. Stone, A.J. Coury, R. Weissleder, R. Langer, D.G. Anderson, Painting blood vessels and atherosclerotic plaques with an adhesive drug depot, Proc. Natl. Acad. Sci. U. S. A. 109 (2012) 21444–21449.